

Thermo-photovoltaic spacecraft electricity generation

A. Kovacs¹ and P. Janhunen²

¹BroadBit, Espoo, Finland

²Finnish Meteorological Institute, Helsinki, Finland

Received: 29 October 2009 – Revised: 4 June 2010 – Accepted: 22 June 2010 – Published: 26 July 2010

Abstract. We describe a solution for powering a spacecraft in the 5 kW – 0.5 MW power range. The introduced thermo-photovoltaic electricity generation works without magnets or external cooling; it combines operational simplicity with a good power per mass ratio. Once in orbit, the system shall be capable of powering numerous successive missions within the solar system or a long range exploratory mission.

1 Introduction

This section describes a high-temperature heat source, powered by a beta-decaying isotope. This heat source is essentially a hot sphere, which will be surrounded by the thermo-photovoltaics. The requirements on the ideal radio-isotope are the following:

- decays without too much gamma or neutron emission, so that no shielding would be required
- it has a long half-life of several years or decades, so that extended missions are supported
- high decay energy per isotope mass

The Sr₉₀ isotope meets these requirements; it decays with a 28.8 years half-time through the following beta-decay process: Sr₉₀ → Yr₉₀ → Zr₉₀.

The total average energy release of the above decay process is 1.14 MeV (Doseinfo, 2010). As calculated in the following sections, the emerging bremsstrahlung radiation is mostly absorbed in the core itself. Sr₉₀ can be produced in large quantities as an output of fission reactors; it is 4.5% of the fission yield in U₂₃₅ fissioning reactors, and there would

be even higher yield of this isotope in Thorium breeder reactors. An industrial process for its separation from the nuclear waste has been described (Law et al., 2006). In fact over 3.5 tons of Sr₉₀ has been used for powering Soviet-era arctic lighthouses in the 1980s. Therefore Sr₉₀ is a suitable candidate isotope.

A high temperature of the heat source is needed for efficient photovoltaic conversion. As a first factor, the temperature depends on the ratio of core mass and surface area, as the produced heat power is proportional to the Sr₉₀ mass. It is therefore preferable to use SrO; a minor addition of oxygen mass significantly increases the core density to 4.7 g/cm³. The other factor that determines the emissivity is the surface material of the radiating core. The temperatures as a function of core mass are shown in Fig. 1 for different constant emissivity values, obtained from the Stefan-Boltzmann law. This core will be surrounded by a photovoltaic sphere, where a high-pass filter reflects back sub-bandgap wavelength radiation. These reflections further contribute to the increase in core temperature. The compound effect of a reduced core emissivity and an efficient optical filter can result in very high core temperature values. If the temperature of a solid SrO core were to turn out too high, it could be easily reduced by decreasing the core density.

Three different core surface types will be investigated:

- a Tungsten surface, which has a moderate emissivity. Its emissivity spectrum data is taken from (Touloukian et al., 1970).
- an Erbium-based surface layer described in (Diso et al., 2003), which has low emissivity except for the emission peak at 1530 nm. This peak makes it particularly useful for frequency matching with 0.7 – 0.8 eV bandgap photovoltaics.
- a SiC surface, which has a relatively constant 0.85 emissivity value in the frequency range of interest.



Correspondence to: A. Kovacs
(andras.kovacs@broadbit.com)

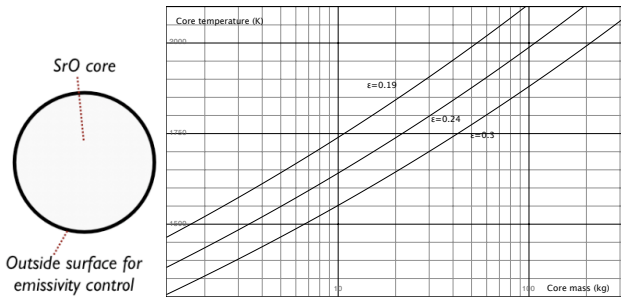


Fig. 1. Cross section of the isotope heat source and its temperature for various surface emissivity values.

With the above arrangement, the core maintains its temperature for over a century in a useful range for high-efficiency thermo-photovoltaic conversion. The overall weight of the radioisotope core can range anywhere from a few kg to some tons; its actual weight would be adjusted for the mission requirements. Subsequently to the propulsion phase, the radioisotope core maintains sufficient temperature for several centuries to power the instruments of the space-craft.

During launch the core is supported by heavier struts which provide mechanical stability and conduct away heat. For the operational configuration which is arranged in orbit, thin rods are enough to keep it at the center of the surrounding photovoltaic sphere. For safety reasons, it may be decided to use SrF_2 core material instead of SrO ; such substitution would result in a minor change of the power-per-mass ratio. An advantage of SrF_2 is that it is not soluble in water which is relevant for eliminating contamination hazard in case of an accident.

2 Thermo-photovoltaic power generation

A number of concepts have been proposed for on-board heat-to-electricity conversion which are reviewed in this section. This establishes the state of the art which will be significantly surpassed by the proposed thermo-photovoltaic generator.

One prototype design is the Stirling-engine converter (Schmidt, 2003). The prototype converter design described in this reference provides 3.2 We/kg, and has a conversion efficiency of 20 – 24%. An alternative mechanical design is the Brayton-cycle engine, which has been planned for the recently cancelled Jupiter Icy Moon Orbiter (JIMO) mission. The overall design has involved an on-board nuclear reactor with a 100 kW Brayton-cycle power conversion system and extensive cooling panels. This converter design has a planned performance of 36 We/kg. A disadvantage of both of these designs is that they introduce vibration of the spacecraft, which may interfere with the operation of some sensors.

It has been previously anticipated that high-powered electricity generation in space would take place through the use of MHD generators (Anghaie, 2002). Besides equipment

complexity, the main disadvantage of MHD generators is the requirement of high magnetic fields at the hot MHD plasma, which requires cooling of the magnets to lower temperature and thus adds significantly to the engine weight.

Thermophotovoltaic electricity generation presents an alternative approach. The proposed thermo-photovoltaic generator works on the principle of a spherical thermal radiation emitter which is surrounded by a larger spherical photodiode layer. Such power generation has potentially a rather high efficiency. It is mostly advantageous for the reasons of reduced weight, operational simplicity and the capability to directly provide high-voltage DC output. Its efficiency is determined by the relative sizes of the core and photovoltaic surfaces, the arrangement of the reflective filter in front of the photovoltaics and the structure of the photovoltaics. The following paragraphs analyze these components in order to compare its resulting power-per-mass ratio against the performance of the above mentioned other technologies.

This section considers traditional photovoltaic material, while the following section describes the strategy for optimizing the photovoltaic structure for space propulsion. Because of the spherical arrangement, the majority of radiative electron-hole recombination is captured in some other part of the photovoltaic sphere, which results in higher efficiency than in case of traditional flat-surface photovoltaics. Therefore, direct bandgap semiconductors are favored. The numeric details of this effect depend on the specifics of the photovoltaic structure; this section makes a conservative estimate by not considering new distant electron-hole pairs generated after radiative recombination. The choice of photovoltaic band-gap always represents a trade-off between the intensity of received useful radiation and the temperature sensitivity of the photovoltaic film.

Without a filter on the photovoltaic side, below-bandgap photon energy would be lost energy. It is advantageous to use a highly reflective tandem-filter (Fourspring et al., 2006) before the photovoltaic junction for reflecting back the long-wavelength spectrum, which will be then absorbed at the thermal radiator. A tandem filter consists of two layers; a photonic surface for reflecting back 2 – 6 micron wavelength photons, and a plasma filter for reflecting back 6 – 10 micron wavelength photons. By adjusting the layer thickness of the photonic structure, the limit of reflecting range can be tuned to match the bandgap of the photovoltaic component. Figure 2 shows the reflectivity of such filter. It has been measured to reflect back 95% of below-bandgap radiation. This ratio may improve in the near future because of improving photonic surface fabrication capability. Furthermore, the measurement of this below-bandgap reflectivity in (Fourspring et al., 2006) has been with an angle of incidence distribution of an omnidirectional source, while in our case the angle of incident is always nearly perpendicular which is optimal for the operation of the photonic interference filter. Therefore measurements results from (Fourspring et al., 2006) can be used as a conservative estimate.

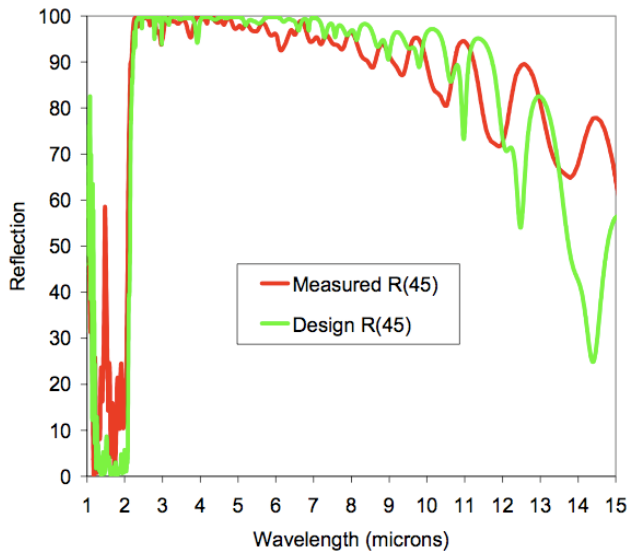


Fig. 2. The reflectivity of tandem-filter, reproduced from (Fourspring et al., 2006).

A crucial issue is the direction of reflected radiation. Since the hot surface and the photovoltaic sphere are concentric, reflected photons will be concentrically converging onto the hot surface when reflection is scatter-free, even though the reflector surface area is much larger than the radiator surface area. This can be easily seen by a geometric argumentation. At any point on the outer sphere, the perpendicular direction is pointing to the sphere's geometric center. Both the interference filter and the photonic filter consist of surfaces that are smooth with respect to the infrared wavelength; for non-perpendicular photons the angles of incidence and reflection are therefore the same. Because of spherical symmetry, if a photon has been emitted from the inner radiator sphere, it will hit that sphere again after reflection. High smoothness of reflector surface is therefore a requirement for enabling re-absorption with only few reflections. Taking the current 95% reflection capability for conservative estimate, the loss ratio of below-bandgap photons at the filter - resulting from back-and-forth radiation between filter and core - is $0.05 \times (1 - 0.95 \times (1 - \epsilon))^{-1}$, where ϵ is the emissivity of the radiator core. Regarding above band-gap photons, 3% filter absorption has been found in (Fourspring et al., 2006).

The photovoltaics is kept at such distance from the radiator that its temperature will permit a reasonable conversion efficiency and limited weight. Larger distance is useful for keeping photovoltaic temperature low and thereby increasing the system efficiency. However the mass of the photovoltaic sphere grows with increasing radius. The output voltage is adjusted through the ratio of serial / parallel connected photovoltaic tiles. This output voltage level may be set to a few thousand volts so that electric wiring does not contribute significant additional weight. A subsequent DC-DC down-

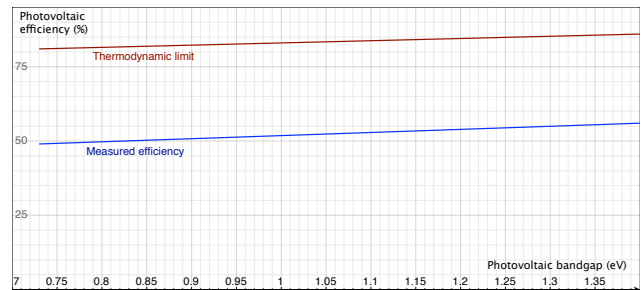


Fig. 3. Measured monochromatic photovoltaic efficiency of a single surface and its theoretical limit.

conversion stage would be added in case of some propulsion methods - such as MPD thrusters - that require lower voltage input power. Such downconversion can be about 90% efficient, which must be taken into account for overall system efficiency.

A reasonable photovoltaic sphere temperature is 300 to 400 K. An overall conversion efficiency estimation must account for the effects listed below; the significance of each effect depends on the choice of system parameters:

- 12% – 25% radiated photon loss in the reflector layer
- 17% – 30% of photon energy is lost because of the mismatch between average photon energy and bandgap energy. This ratio is calculated from the thermal radiation spectrum that reaches the photovoltaic layer past the filter.
- The feasible thermodynamic limit of photovoltaic conversion efficiency and the measured efficiency at room temperature under exact wavelength match condition (Andreev et al., 2003) are shown on Fig. 3. The temperature dependence of this conversion efficiency depends on the photovoltaic bandgap.

The theoretical temperature dependence of photovoltaic efficiency for the case of solar illumination is described in (Landis et al., 2004; Sanders, 2007), and is summarized in Fig. 4. The rate of efficiency drop per kelvin is nearly constant during the bulk of efficiency degradation. While the two referenced temperature dependence estimates differ substantially, their difference makes only a small impact on the final outcome.

Furthermore, because of the thermal radiation's 4th power dependence on surface temperature, the mass of the photovoltaic sphere mainly depends on its temperature. A change in photovoltaic temperature significantly affects the power per mass ratio.

In order to find an optimum energy conversion system, the following analysis will investigate heat-to-electricity conversion efficiency in terms of photovoltaic temperature, the photovoltaic band-gap, and the material choice of the core surface.

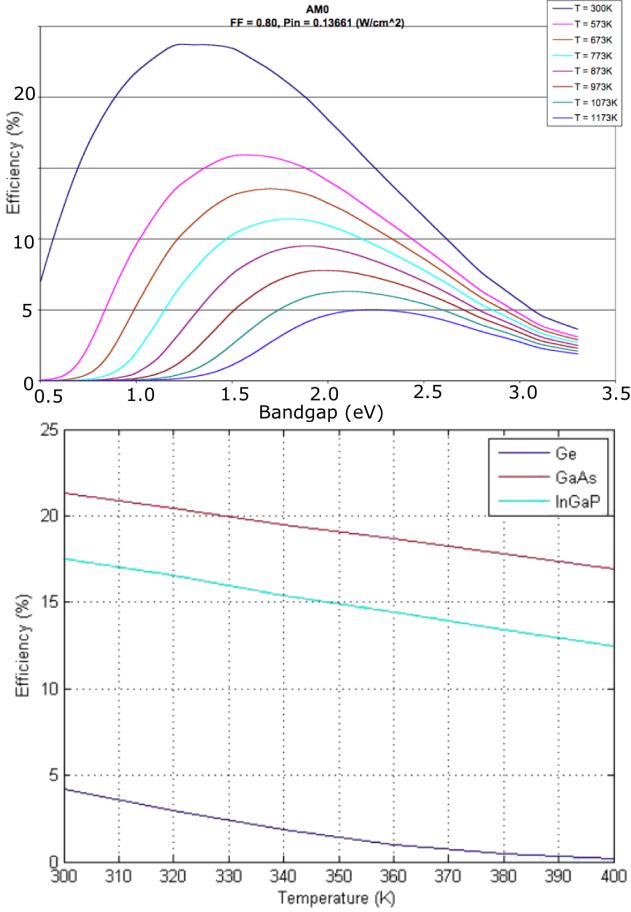


Fig. 4. Photovoltaic solar conversion efficiency in terms of photovoltaic temperature; optimistic and pessimistic numeric simulations. Reproduced from (Landis et al., 2004) and (Sanders, 2007).

Using the calculation method outlined above, Table 1 lists the achievable conversion efficiency in terms of system parameter choices. The listed core temperatures are feasible for all core weights starting from 100 kg.

The indicated 2000 K temperature limit is justified by showing that it allows for a long term operation with Tungsten surface, while a hotter surface may potentially limit the photovoltaic lifetime. The evaporated core surface material will eventually deposit over the photovoltaic surface. It must be ensured that such condensation would not change the optical properties of photovoltaic surface during the spacecraft lifetime.

Tungsten's vapor pressure at 2000 K is 2×10^{-10} Pa. The corresponding particle density near the hot surface is $n = (p_{\text{vapor}}/k_b T)$. From kinetic gas theory, the flux of evaporated particles at the core surface is $\phi_{\text{core}} = n \sqrt{k_b T} / 2\pi m$. At photovoltaic surface this flux is reduced by the ratio of these inner and outer surfaces, which is calculated from the

Table 1. Heat to electricity conversion efficiencies. The shaded rows indicate calculations based on pessimistic photovoltaic temperature dependence.

Core surface	Core temp.	Effective emissivity	PV temp.	Optimal bandgap	Conversion efficiency
Tungsten	2000 K	13%	300 K	0.8 eV	28.4%
Tungsten	2000 K	11%	400 K	0.9 eV	20.9%
Er ₃ Al ₅ O ₁₀	1500 K	12%	300 K	0.7 eV	29.2%
Er ₃ Al ₅ O ₁₀	1500 K	12%	400 K	0.7 eV	19.9%
SiC	1500 K	19%	300 K	0.7 eV	30.1%
SiC	1500 K	19%	400 K	0.7 eV	20.5%

thermal emission law:

$$\phi_{PV} = \phi_{\text{core}} \frac{A_{\text{core}}}{A_{PV}} = \phi_{\text{core}} \left(\frac{T_{PV}}{T_{\text{core}}} \right)^4 \frac{\epsilon_{\text{blackbody}}}{\epsilon_{\text{core}}}.$$

At 400 K photovoltaic temperature this flux is approximately $10^6 \text{ s}^{-1} \text{ cm}^{-2}$. The allowed deposition thickness is an order of magnitude less than the relevant optical wavelength, and is therefore limited at 0.2 microns. Taking a worst case assumption of having all the atoms from the incoming flux to stick to the surface, it takes about 100 years to accumulate a 0.2 microns thick metal layer over the photovoltaics, making 2000 K a suitable operating temperature for the Tungsten covered core.

With only 4% temperature increase, Tungsten's vapor pressure grows 10-fold. Since the vapor flux primarily depends on this pressure change, the core should not be operated at higher temperatures if Tungsten's sticking coefficient is near unity. Even the case of a low sticking coefficient allows only few hundred K increase of the core temperature. Because the vapor pressure values for the other surface materials are not known, the efficiency calculations use 1500 K operating temperature for these materials.

It is then concluded from the data of Table 1 that the achievable conversion efficiency is 30.1% for the case of 300 K photovoltaic temperature. Taking the average between optimistic and pessimistic estimates at 400 K photovoltaic temperature, the achievable conversion efficiency is 19.2% in that case.

The thickness of the photovoltaic sphere can be very slim; there is nearly no mechanical strength requirement as it is floating in space. The photovoltaic heterostructure, reflective filter, and outside black-body emitter layers are thin films. The photovoltaic structure can be grown over an Aluminum layer, which has 2.7 g/cm^3 density. The thickness of the sphere's material is estimated to be about 0.5 mm, constrained by mechanical strength limit. The comparison of resulting photovoltaic sphere masses is listed in Table 2.

It is seen from above mass and conversion efficiency values that in case of 400 K photovoltaic temperature the power/mass ratio is just 4% better than in the case of 300 K

Table 2. Mass and size of the photovoltaic sphere.

Core mass and thermal power	Mass and radius of the PV sphere at T=300 K	Mass and radius of the PV sphere at T=400 K
100kg, 80 kW _{th}	162 kg, 3.1m	60 kg, 1.9m
500kg, 400 kW _{th}	810 kg, 6.9m	300 kg, 4.1m
2000kg, 1.6 MW _{th}	3240 kg, 13.8m	1200 kg, 8.2m

photovoltaic temperature. The achievable power/mass ratio is about 100 W/kg when considering the whole power source, and 263 W/kg when considering just the heat to electricity conversion.

The effective surface emissivity listed in Table 1 is a rather low value because of the reabsorption of radiation that is reflected back by the tandem filter. As a result, it can be seen from Fig. 1 that even a very small core mass is sufficient for achieving the target core temperature. The minimum generator size limit is therefore set not by the temperature requirement, but by the radiation tolerance requirement, which will be analysed next.

Sun-powered space photovoltaics' gradual degradation is caused by a number of factors. These factors apply only to a limited extent to our thermo-photovoltaics:

- UV-induced degradation: prevented by the outside layer
- Sputtering of translucent surface by solar wind plasma: prevented by the outside layer
- Collision with micro-meteorites and debris: partly applies, as the outside layer protects only against smallest meteorite particles
- Damage from high-energy radiation applies as with ordinary solar panels.

An important consideration is the photovoltaics' tolerance of gamma-rays produced by the radio-isotope core itself. The effect of 1 MeV electron bombardment on GaAs photovoltaics is described in (Pinzon, 1991). In that study an electron fluence of 10^{15} cm^{-2} caused the produced power to degrade to 75% of its original value. Furthermore it was found that a thermal annealing applied at just 360 K temperature has mostly restored the output power to its original value, with successive irradiation and annealing cycles showing similar results. This temperature is a feasible operating temperature for the thermo-photovoltaics considered in this paper. Moreover, since the melting point of GaSb is significantly lower than GaAs melting point - 985 K vs. 1511 K - it is reasonable to assume similar thermal recovery performance of GaSb already at 300 K temperature. Therefore the photovoltaics is estimated to have only minor performance degradation up to an absorbed gamma ray fluence of $5 \times 10^{15} \text{ cm}^{-2}$ in the 1 MeV energy range. A reasonable

operational requirement is to have the total absorbed fluence within this limit for the duration of Sr₉₀ half-life. Let us estimate the gamma radiation fluence for a 500 kg SrO core. The following factors multiply to produce the total fluence value:

- The number of decay events per photovoltaic cm^2 . This value is 10^{21} cm^{-2} during the Sr₉₀ half-life.
- The gamma ray absorption ratio in the photovoltaics. While the photovoltaics can be much thinner than the 200 micron thick samples used in (Pinzon, 1991), the same thickness value is used here for compatibility of results. While the absorption is less a thinner photovoltaics, the relative significance of each defect is larger. The absorption ratio is 6×10^{-3} for 1 MeV photons and 1.6×10^{-2} for 0.1 MeV photons.
- The gamma ray absorption rate in the SrO core. In order to escape the core, a photon has to travel approximately an average distance of the core radius, which is 30 cm. Based on a Monte-Carlo simulation, the rate of escaping radiation is 7.5×10^{-3} for 1 MeV photons and 2.2×10^{-4} for 0.1 MeV photons.
- The spectrum of bremsstrahlung photons. The shape of this spectrum makes only a minor difference. By multiplying the above loss and absorption factors, the difference between one 1 MeV photon and ten 0.1 MeV photons amounts to only a factor of 2.
- The ratio of beta electron energy, which turns into bremsstrahlung. According to (Turner, 2007), ratio of radiative to collisional electron energy dissipation can be approximated by the $Z \times E/800$ formula, where Z is the atomic number and E is the initial electron energy expressed in MeV. Based on this formula, just 2.7% of the beta decay in SrO is dissipated as bremsstrahlung.

By multiplying through above factors, the total 1 MeV energy equivalent gamma ray fluence that the photovoltaics receives during 30 years is 10^{15} cm^{-2} , which can be tolerated without a significant performance degradation. There is a 25% anticipated power loss during this time without a thermal recovery effect, and only a few percent power loss in case of a suitably chosen photovoltaics material, such as GaSb. Consequently, the proposed system appears suitable for long-term space missions, even without an added radiation shielding.

The received radiation fluence reaches the $5 \times 10^{15} \text{ cm}^{-2}$ limit when the rate of escaping radiation becomes 5 times as much as in the previous example. From Monte-Carlo simulation, this limit is reached at a core mass of 66 kg; some radiation shielding must be used for smaller core masses. A reasonable lower mass limit is the point at which the mass of shielding is around the same as the core mass itself. This limit is reached with a core mass of 20 kg. The corresponding

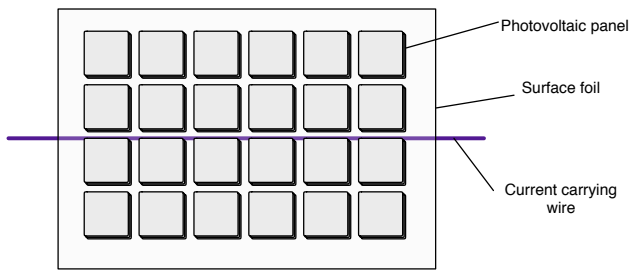


Fig. 5. Structure of the photovoltaic sphere.

electricity generation is 5 kW, which is taken as the approximate lower limit of this concept's output scaling.

The surface of both the thermal radiator and the photovoltaic components will be made out of many tiles, as shown in Fig. 5. The foil is compactly packed for the launch operation. Once in orbit, the rocket will start spinning around its axis, and the radial force naturally unpacks the photovoltaics into spherical shape. There are mild forces and no pressure to withstand as long as the rocket is in space. A crucial requirement is that the reflective tandem-filter must survive the launch and unpacking operations. This requirement can be met for example by applying enough pressure during the packed stage for the tiles would not to move relative to each other. Additionally, a thin protective diamond layer can be uniformly deposited on top of the filter surface.

The ideal material for the outside photovoltaic surface acts as a black-body in the relevant thermal spectrum, but becomes highly reflective in the visible and UV spectrum. Solar heating effects are then negligible even at 1 AU distance from the Sun. This desired property is met by some metal oxides. Al_2O_3 is for example highly emissive for larger than 5 micron wavelengths and highly reflective for smaller than 3 micron wavelengths.

Whether the tiles can be planar or whether they must be curved depends on their size relative to the core radius. In case of a planar tiles the divergence of reflected photons from of their desired path can be up to the width of a tile. So the size of planar tiles should be about an order of magnitude less than the core radius size in order to avoid significant additional reflections.

The unpacking of the photovoltaic sphere in orbit can be designed for example along the following procedure:

1. The spacecraft begins spinning and the tiles extend from the packing as radial surfaces near one axial end of the sphere.
2. The hot core is moved into the center of the sphere by thin rods.
3. Mechanized 'zips' slide along the edges of the segments of tiles and close the photovoltaic surface into a sphere.

Current nano-fabrication techniques make the production of required tiled thin-film structure feasible at specialist institutions.

3 Optimization of the photovoltaic structure

While the previous section estimated the achievable conversion efficiency with generic photovoltaics, this section outlines the strategy for optimizing the photovoltaic structure. Losses are caused by thermal relaxation of generated electron-hole pairs and non-radiative Auger recombination of electron-hole pairs. Radiative recombination of electron-hole pairs only indirectly contributes to losses, by increasing the distance that radiation travels in the filter before generating a non-recombining electron-hole pair.

A main criterion for optimizing the power/mass ratio is the improvement of photovoltaic temperature tolerance. The temperature tolerance can be firstly improved by thinning the photovoltaic structure, so that generated electron-hole pairs have less distance to travel to the heterojunction.

A simple layer thinning would however mean increased attenuation, as photons would have to travel multiple passes before generating electron-hole pairs. Two possible strategies for achieving light absorption at shorter distances are the following:

- Use of some new type of photovoltaics material, which results in better absorption than presently used infrared photovoltaics materials. The Microcrystalline Germanium Carbide material described in (Dalal et al., 2001) is a potential candidate material.
- Nano-patterning of the photo-voltaic surface. Combining photovoltaics with a sub-wavelength nano-patterned structure, such as described in (Diem, 2009), results in efficient trapping of incoming radiation even for very thin photovoltaic layers.

The rate of radiative and non-radiative recombinations also depends on the doping concentrations, which becomes a further optimization parameter as radiative recombination mostly causes new electron-hole pairs in some other part of the photovoltaic sphere. In summary, making photovoltaics operation more tolerant of high temperatures is an optimization process on the combination of following parameters:

- the thickness of the photovoltaic layer, where electron-hole pairs are generated
- the selection of photovoltaic materials
- the applied doping concentration

Considering the 60% difference between current photovoltaic efficiency and its corresponding thermodynamic limit, as well as the possible power/mass ratio improvement

through more heat tolerant photovoltaics, the potential efficiency improvement through the outlined strategy can be substantial.

4 Enabled spacecraft performance

A possible utilization of thermo-photovoltaically generated electricity is the powering of instruments in outer solar system missions. The availability of high electric power allows the operation of high-resolution telemetry instruments, including power-intensive radar measurements. The rate of streamed telemetry data would not be limited by power considerations. An example of such missions is the previously mentioned JIMO mission for the exploration of Jupiter's moons. This mission would have been also searching for signs of life in the subsurface oceans of these moons. Its design has involved an on-board nuclear reactor with a 10 kW_e Brayton-cycle power conversion system. The planned weight of this conversion system has been 2.8 tons. The thermo-photovoltaic electricity generators described in this article can provide a simpler and more compact solution for generating this amount of electric power, requiring a total photovoltaic weight of 390 kg for the same output power. The weight of described heat-to-electricity conversion components is therefore just 14% of the Brayton-cycle power conversion system weight that has been planned for the JIMO mission. Furthermore, the complementing 650 kg SrO core has a similar mass to a light-weight nuclear reactor.

Thermo-photovoltaic electricity generation can power a number of propulsion methods, such as magnetoplasmadynamic (MPD) thrusters, magnetic solar sails (Zubrin, 1993), electric solar sails (Janhunen et al., 2007), and other future technologies. The analysis from previous sections has shown that with traditional photovoltaics the expected fuel-less and payload-less rocket weight could be in the range of 75 kg – 3.2 tons corresponding to 5 kW – 310 kW generated electric power. The highest-power option is beneficial for time-constrained missions to nearby planets. The lower-power option is beneficial for weight-constrained missions and for long range missions.

While MPD propulsion is a matching near term option, it would be eventually replaced by propulsion techniques that use input electric power more efficiently. Field Emission Electric Propulsion (FEEP) thrusters (Alta, 2010) and colloid (electro-spray) thrusters (Busek, 2010) offer the combination of highly efficient utilization of input electric power as well as up to 10 000 s Isp values. FEEP thrusters work on the principle of electrostatic acceleration of ions from a liquid metal fuel reservoir, which is typically Cesium. Over 90% thruster efficiency is feasible with this approach. FEEP/colloid thrusters have not yet been designed for propulsion, because a single thruster provides only up to 1 mN thrust force. Such thrusters can, however, be potentially fabricated at micro-meter scales. An array of many

thousands of micro-fabricated FEEP/colloid thrusters will be capable of providing a large overall thrust force, while maintaining low total thruster weight. A further advantage of FEEP/colloid thrusters is that they use few thousand volts of DC input voltage, thereby avoiding the need for voltage downconversion. In summary, a heat-to-thrust efficiency of 18 – 27% becomes possible with the use of FEEP/colloid propulsion. For exploratory missions, the final rocket speed estimation is made for a payload mass of 300 kg and the electricity generator weighing 1.3 tons, which provides 125 kW electric output. Assuming a 6 ton initial rocket mass, a final rocket speed of over 130 km/s can be achieved in less than 6 years.

With future improvements in the temperature stability and spectral efficiency of tandem-filters, higher photovoltaic operating temperature would become possible. The use of custom-designed photovoltaics, which has been outlined in this paper, will increase the power per mass ratio and the feasible rocket performance even further.

Edited by: H.-J. Fahr

Reviewed by: two anonymous referees

References

- Alta: <http://www.alta-space.com/index.php?page=feep>, access: 20 June 2010.
- Andreev, V., Khvostikov, V., Kalinovsky, V. et al: High current density GaAs and GaSb photovoltaic cells for laser power beaming, Proc. of 3rd World Conf. on Photovoltaic Energy Conv., 2003.
- Anghaie, S.: Development of Liquid-Vapor Core Reactors with MHD Generator for Space Power and Propulsion Applications, Final report of DOE project DE-FG07-98ID 13635, 2002.
- Busek: <http://www.busek.com/colloid.html>, access: 20 June 2010.
- Dalal, V. and Herrold, J.: Microcrystalline Germanium Carbide: A new, almost direct gap, thin film material for photovoltaic energy conversion, Materials Res. Soc. Symp., A25.12, 2001.
- Diem, M.: Wide-angle perfect absorber/thermal emitter in the terahertz regime, Phys. Rev. B, 33 101–33 104, 2009.
- Diso, D., Licciulli, A., Bianco, A. et al.: Selective Emitters for High Efficiency TPV Conversion: Materials Preparation and Characterisation, AIP Conf. Proc., 132–141, 2003.
- Doseinfo: <http://www.doseinfo-radar.com/RADARDecay.html>, access: 20 June 2010.
- Fourspring, P. M. and DePoy, D.: Spectral Control for Thermophotovoltaic Energy Conversion, KAPL Inc. report ARP-AC-1326-PMF-E1, 2006.
- Janhunen, P. and Sandroos, A.: Simulation study of solar wind push on a charged wire: basis of solar wind electric sail propulsion, Ann. Geophys., 755–767, 2007.
- Landis, G., Merritt, D., and Reyne, R.: High-Temperature Solar Cell Development, 19th Europ. Photovoltaic Science and Engineering Conf., 2004.
- Law, J. D., Herbst, R., Peterman, D. et al.: Development of Cesium and Strontium Separation and Immobilization Technologies in Support of an Advanced Nuclear Fuel Cycle, Waste Management'06 Conf. Proc., 2006.

- Pinzon, D.: Analysis of radiation damaged and annealed Gallium Arsenid and Indium Phosphide solar cells using deep level transient spectroscopy techniques, Master's Thesis, 1991.
- Sanders, M.: Modeling of operating temperature performance of triple junction solar cells using Silvaco's Atlas, Master's Thesis, 2007.
- Schmidt, G.: Radioisotope Power Systems (RPS) for New Frontiers Applications, present. at the NASA New Frontiers Prog. conf., 2003.
- Touloukian, S. and DeWitt, D.: Thermal Radiative Properties - Metallic Elements and Alloys, IFI/Plenum, New York, USA, 1970.
- Turner, J. E.: Atoms, Radiation, and Radiation Protection, Wiley-VCH, Weinheim, Germany, 2007.
- Zubrin, R.: The use of magnetic sails to escape from low earth orbit, J. of the Brit. Interpl. Soc., 46, 3–10, 1993.